VOLUME 4, NUMBER 1, JANUARY 2004

NANO LETTERS

Local Gating of Carbon Nanotubes

M. J. Biercuk, N. Mason, and C. M. Marcus*

Department of Physics, Harvard University, Cambridge, Massachusetts 02138

Received August 24, 2003; Revised Manuscript Received October 30, 2003

ABSTRACT

Local effects of multiple electrostatic gates placed beneath carbon nanotubes grown by chemical vapor deposition (CVD) are reported. Single-walled carbon nanotubes were grown by CVD from Fe catalyst islands across thin Mo "finger gates" (∼150 nm × 10 nm). Prior to tube growth, several finger gates were patterned lithographically and subsequently coated with a patterned high-κ dielectric using low-temperature atomic layer deposition. Transport measurements demonstrate that local finger gates have an effect that is distinct from that of a global backgate.

Considerable effort has been focused on incorporating single-walled carbon nanotubes (SWNTs) into nanoscale analogues of solid-state electronic devices. SWNT transistors have been realized,[1−3] as have nanotube circuits exhibiting more subtle features such as Coulomb charging and the Kondo effect.[4−6] To fully explore the richness of nanotube device physics, independent control of relevant physical parameters is required. Many of these features may be controlled by electrostatic gating, in which the SWNT device is capacitively coupled to one or more nearby gate voltages.

There have been a number of recent advances in gating of SWNT devices, including the use of Al backgates with thin oxide layers,[7,8] the use of high-κ dielectrics,[9] metallic side gates,[10] liquid-phase electrolyte solutions,[11] and external scanned gates.[12−14] However, a technique for implementing local gating via standard lithography in devices utilizing chemical vapor deposition (CVD) nanotube growth has not yet been presented to our knowledge. In previous work, nanotube devices with multiple electrostatic topgates[9] or a metallic gate underneath the nanotube[15] were fabricated to produce multigate devices, including OR logic transistors. In these cases, however, data appeared consistent with a global coupling of all topgates. More recently, experimental work has also indicated that it is possible to gate spatially localized sections of a nanotube device.[16] This work focused specifically on gate control over room-temperature SWNT-based field effect transistors fabricated using random nanotube deposition, however.

In this letter we report a technique for achieving local control of CVD-grown nanotube conduction via multiple electrostatic gates. Device fabrication is based on growth of SWNTs from Fe catalyst and takes advantage of two notable processing features: (1) thin Mo "finger gates" (∼150 nm wide), robust against the CVD process, are defined lithographically, allowing nanotubes to be grown across them; and (2) a high−κ dielectric layer is patterned by photolithography and a liftoff procedure using low-temperature atomic layer deposition (ALD).[17] Transport data from a nanotube device fabricated in this manner indicate that the effect of individual finger gates is qualitatively different from that of a global backgate.

Devices were fabricated on doped Si wafers with 1 μm of thermally grown oxide as a base substrate, allowing the conducting Si to be used as a global backgate. Before nanotube growth, sets of five parallel Mo finger gates roughly 150 nm wide and < 10 nm thick, spaced by ∼400 nm,

* Corresponding author.

10.1021/nl034696g CCC: $27.50
Published on Web 11/19/2003

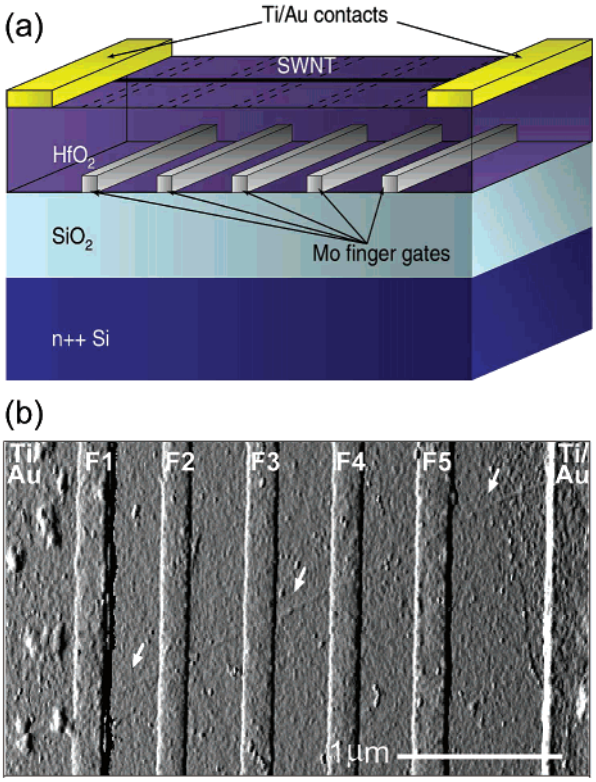

Figure 1. (a) Schematic of finger gated devices. Mo gates (150 nm wide × 10 nm thick) were defined lithographically on a Si/SiO_2 substrate and subsequently coated with ~25 nm of HfO_2 grown by low-temperature ALD. Nanotubes were grown across these local gates by CVD and contacted with Ti/Au electrodes. Not to scale. (b) Atomic force micrograph of nanotubes grown across Mo finger gates and contacted (far left and far right) by Ti/Au leads. Note that one finger gate passes directly underneath the nanotube−metal contact. Arrows indicate the location of the nanotube. Finger gates are labeled as in the text.

extending approximately 100 μm in length (Figure 1a) were patterned using electron-beam lithography liftoff and deposited using electron-beam evaporation. Larger Mo lines connected to the fine Mo gates were then patterned with photolithography liftoff.

Mo was chosen for its tolerance to the high temperatures and reducing atmosphere used in CVD processing, combined with reasonably low resistivity in thin-film form. Similar conclusions favoring Mo for this purpose were reached independently in ref 18. Thin gate metallization (<10 nm thickness) was used to avoid bending defects created by a nanotube "draping" over raised contacts.[19] We found that 5 nm films of Mo exposed to CVD processing vanished, while thicker layers remained intact (minus ~5 nm). Thus, metal that was exposed to the CVD environment always included a sacrificial layer of ~5 nm.

After fabrication, the finger gates and their connections were covered by 25 nm of HfO_2, deposited using low-temperature ALD and patterned using photolithography and liftoff.[17] The dielectric layer was patterned to form large mesas that covered the finger gates but left the contacts exposed, as shown in Figure 2. Next, rectangular patterns (~1 μm × 5 μm) were defined in a poly(methyl methacrylate) (PMMA) layer using electron-beam lithography, and ~1

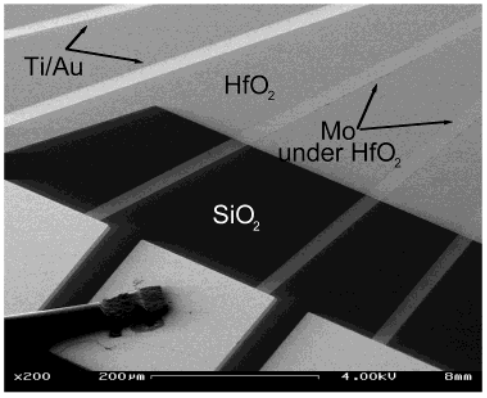

Figure 2. Scanning electron micrograph showing liftoff-patterned ALD oxide mesa edge (middle) showing Ti/Au wires on top of the mesa (upper left) and Mo wires running underneath the patterned ALD (bottom).

nm Fe was deposited using thermal evaporation. The rectangles were oriented in rows on either side of the Mo finger gates and served to locate the Fe catalyst to promote nanotube growth across the underlying finger gates. A standard CVD recipe using methane as a carbon source was employed for tube growth,[20] after which SWNTs crossing the finger gates were located using an atomic force microscope (AFM).[21] Finally, SWNTs were contacted with Ti/Au contact pads to complete the devices (Figure 1b). Typical device dimensions (between contacts) were 3−5 μm. Atomic force and (post-measurement) scanning electron microscopy ensured that the finger gates were continuous.

Transport measurements were made at 4 K using a dc voltage bias, $V = 10$ mV, and measuring dc current, I.[22] Data are presented for a single device (Figure 3); similar behavior was observed for other devices. Conductance, $G = I/V$, was measured as a function of voltages applied to various finger gates and the backgate. Sweeping the backgate with the finger gate voltages held fixed at 0 V produces rapidly varying, reproducible fluctuations in G as a function of backgate voltage, V_B (Figure 3b). The $G(V_B)$ data show that the SWNT is likely metallic, as there is no significant trend in conductance peak height as we move from positive to negative values of V_B. The rapid fluctuations are presumably due to Coulomb blockade resulting from quantum dots defined by scattering centers along the tube, although it is unclear if the scattering centers are innate or caused by the presence of the underlying finger gates. The lack of symmetry within the Coulomb fluctuations is consistent with the presence of multiple quantum dots in series. The backgate seems to couple to all of these dots simultaneously and is capable of rearranging charges between the dots.[14]

Sweeping the voltage on individual finger gates produces qualitatively different behavior in the conductance. In this case, we observe smooth changes in G as a function of all of the finger gate voltages (Figure 3a). One of the gates (F5) exhibits a broad resonance feature. Setting a single finger gate to a nonzero voltage, V_F, with the other finger gates held at zero again yields rapid fluctuations in $G(V_B)$, but with different overall amplitude, consistent with the $G(V_F)$ from Figure 3a acting as an overall smooth envelope of $G(V_B)$.

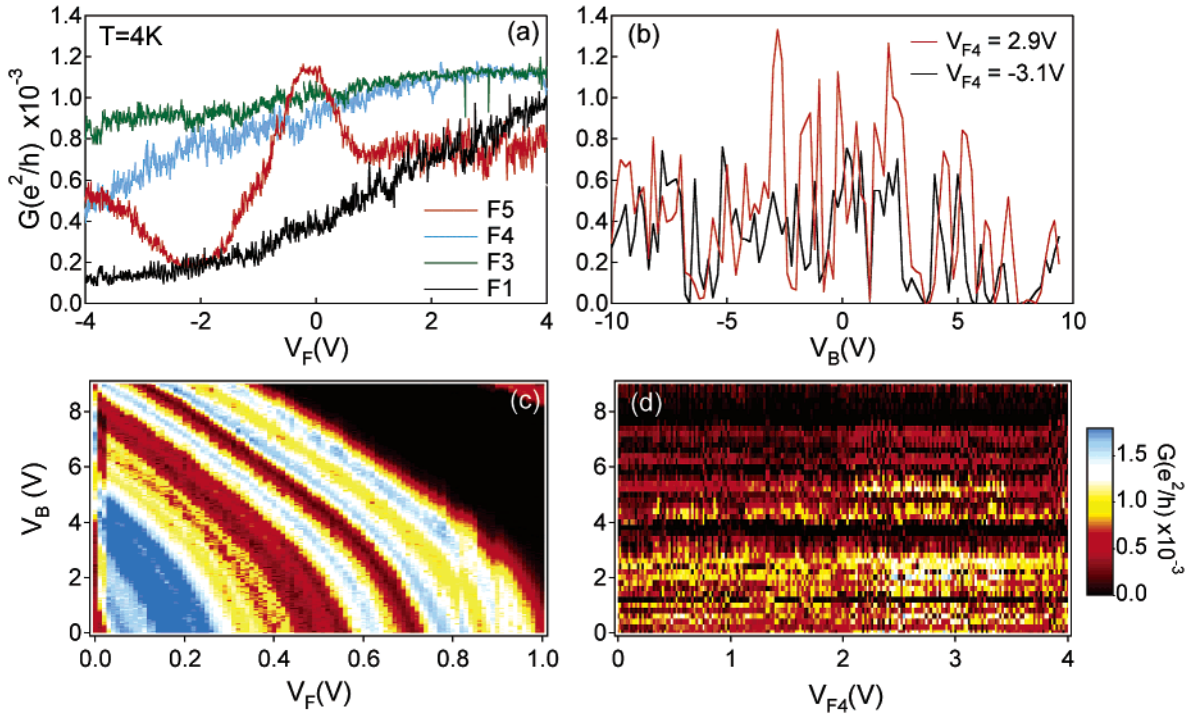

Figure 3. Transport measurements taken from the device depicted in Figure 3. All data taken at 4 K. (a) Conductance as a function of various finger gate voltages. Each trace represents the effect of a single finger gate swept from +4 V to −4 V while all others, including the backgate, are set to 0 V. Gate F2 showed significant leakage above $V_{F2} \sim 2$ V and so was not included in these plots. (b) Charging effects observed by sweeping the Si backgate. Traces are displayed for two different voltages on finger gate F4, which changes the overall magnitude of the rapid fluctuations without changing the qualitative structure. (c) Color plot of conductance as a function of backgate voltage (V_B) and common finger gate voltage (V_F) (i.e., all finger gates swept together) indicating an additive effect of V_B and V_F. Color scale shows conductance in units of e^2/h. (d) Comparable color plot showing conductance as a function of V_B and a *single* finger gate at V_F with other finger gates set to V = 0.

Examples of $G(V_B)$ for two settings of V_F on F4 are shown in Figure 3b; similar behavior was observed with other finger gates.

The qualitative difference between the effects of the backgate and finger gates suggests that the finger gates act to locally tune the transparency of the aforementioned scattering centers. This picture is supported particularly by the nonmonotonic (resonant-like) behavior of $G(V_{F5})$. Local scatterers have previously been linked to the formation of intratube quantum dots[14,23,24] and have been observed by scanned gate measurements[12−14] and electrical-force microscopy.[25] Additonally, gate F1, located under the SWNT-metal contact could be tuning the transparency of the tunnel barrier formed at the metal−nanotube interface. If the finger gates were instead having a global effect and coupling to the entire tube device, one would expect Coulomb-blockade phenomena very similar to those caused by sweeping the backgate, though perhaps on a different overall voltage scale.

Figure 3c shows device conductance as a function of both backgate and finger gate voltages for the case where all finger gates are swept together. Fluctuations in $G(V_B)$ with $V_F = 0$ V previously described appear again but now evolve continuously into oscillations in $G(V_F)$ with $V_B = 0$ V, demonstrating the approximately additive behavior between V_B and V_F when all finger gates are swept. Evidently, when all finger gates are swept, they together do produce an effective global gating effect much like the backgate, albeit on a reduced voltage scale (as expected given the distances and dielectric constants). Thus, although the effect of the individual finger gates is spatially localized along the nanotube, the area of influence appears to be larger than that defined by the physical dimensions of the finger gates. When the gates are utilized simultaneously, the collective area of influence encompasses the entire device.

As a direct comparison, Figure 3d shows corresponding plots when sweeping just one of the finger gates with the other finger gates held at 0 V. In this case, there is no additive effect evident between finger gate and back gate, even over an expanded range of V_F. Horizontal slices of the 2D plot show roughly the same behavior in $G(V_F)$ as observed at $V_B = 0$ V in Figure 3a (ignoring switching noise), while vertical slices show that oscillations in $G(V_B)$ persist for all values of V_F.

In summary, we have demonstrated a method for local gating using finger gates beneath a catalyst-grown single-wall nanotube. The fabrication process takes advantage of robust Mo finger gates and liftoff-patterned dielectric films deposited by low-temperature atomic layer deposition. Future applications of the technique reported include fabricating multigate nanotube FETs or quantum dots with independent control.

Acknowledgment. We thank J. S. Becker for her help with ALD and D. J. Monsma for many helpful discussions.

This work was supported by funding from the NSF through the Harvard MRSEC and EIA-0210736, and the Army Research Office, under DAAD19-02-1-0039 and DAAD19-02-1-0191. M.J.B acknowledges support from an NSF Graduate Research Fellowship and from an ARO Quantum Computing Graduate Research Fellowship. N.M. acknowledges support from the Harvard Society of Fellows.

References

(1) Tans, S.; Verschueren, A.; Dekker, C. *Nature (London)* **1998**, *393*, 49.
(2) Martel, R.; Schmidt, T.; Shea, H. R.; Hertel, T.; Avouris, Ph. *Appl. Phys. Lett.* **1998**, *73*, 2447.
(3) Wind, S. J.; Appenzeller, J.; Martel, R.; Derycke, V.; Avouris, Ph. *Appl. Phys. Lett*. **2002**, *80*, 3817.
(4) Nygard, J.; Cobden, D. H.; Lindelof, P. E. *Nature* **2000**, *408*, 342.
(5) Tans, S. J.; Devoret, M. H.; Dai, H. J.; Thess, A.; Smalley, R. E.; Geerligs, L. J.; Dekker, C. *Nature* **1997**, *386*, 474.
(6) Bockrath, M.; Cobden, D. H.; McEuen, P. L.; Chopra, N. G.; Zettl, A.; Thess, A.; Smalley, R. E. *Science* **1997**, *275*, 1922.
(7) Bachtold, P. H.; Nakashini, T.; Dekker, C. *Science* **2001**, *294*, 1317.
(8) Ishibashi, K.; Suzuki, M.; Ida, T.; Tsuya, D.; Toratani, K.; Aoyagi, A. *J. Vac. Sci. Technol. B* **2001**, *19*, 2770.
(9) Javey, A.; Kim, H.; Brink, M.; Wang, Q.; Ural, A.; Guo, J.; McIntyre, P.; McEuen, P.; Lindstrom, M.; Dai, H. *Nature Materials* **2002**, *1*, 241.
(10) Ishibashi, K.; Suzuki, M.; Ida, T.; Aoyagi, Y. *Appl. Phys. Lett.* **2001**, *79*, 1864.
(11) Rosenblatt, S.; Yaish, Y.; Park, J.; Gore, J.; Sazonova, V.; McEuen, P. L. *Nano Lett.* **2002**, *2*, 869.
(12) Freitag, M.; Radosavljevic, M.; Clauss, W.; Johnson, A. T. *Phys. Rev. B* **2000**, *62*, R2307.
(13) Bockrath, M.; Liang, W.; Bozovic, D.; Hafner, J.; Lieber, C. M.; Tinkham, M.; Park, H. *Science* **2001**, *291*, 283.
(14) Tans, S. J.; Dekker, C. *Nature* **2000**, *404*, 834.
(15) Javey, A.; Wang, Q.; Li, Y.; Dai, H. *Nano Lett.* **2002**, *2*, 929.
(16) Wind, S. J.; Appenzeller, J.; Avouris, Ph. *Phys. Rev. Lett.* **2003**, *91*, 058301.
(17) Biercuk, M. J.; Monsma, D. J.; Becker, J. S.; Marcus, C. M.; Gordon, R. G. *Appl. Phys. Lett.* **2003**, *83*, 2405.
(18) Franklin, N. R.; Wang, Q.; Tombler, T. W.; Javey, A.; Shim, M.; Dai, H. *Appl. Phys. Lett.* **2002**, *81*, 913.
(19) Bezryadin, A.; Verschueren, A. R. M.; Tans, S. J.; Dekker, C. *Phys. Rev. Lett.* **1998**, *80*, 4036.
(20) CVD growth recipe: 30 m temperature ramp from 25 to 900 C with 0.8 standard liters per minute (slm) Ar, 0.1 slm H_2, 15 m growth with 0.1 slm H_2, 1.5 slm CH_4, cool 2 h in 0.75 slm Ar.
(21) Single walled tubes were selected by contacting only tubes with height profiles approximately 1−2 nm in the AFM.
(22) Room-temperature measurements were unfortunately not possible as a result of sample contamination which froze out at low temperatures.
(23) Chico, L.; Lopez Sancho, M. P.; Munoz, M. C. *Phys. Rev. Lett.* **1998**, *81*, 1278.
(24) McEuen, P. L.; Bockrath, M.; Cobden, D. H.; Yoon, Y.-G.; Louie, S. G. *Phys. Rev. Lett.* **1999**, *83*, 5098.
(25) Woodside, M. T.; McEuen, P. L. *Science* **2002**, *296*, 1098.

NL034696G